Table 1 Comparison of characteristic properties of spot and plume modes

Characteristics typical values	Spot	Plume
Appearance	Intense spot within a few mm radius from exit hole	Luminous bluish plume-like region extending from cathode to about two-thirds of distance to anode
Neutral flow, J_{Hg}, equivalent ma	~50 and higher	~50 and lower
Discharge current, J_I, amp	2.0	0.3
Electron to atom ratio, J_I/J_{Hg}	40	6
Discharge voltage, ΔV_I, v	13.5	35
Plasma potential (with respect to cathode),[a] v	11	11
Electron density (0.5 cm from cathode), n_e, electrons/m^3	10^{18}	10^{17}
Electron temperature,[a] V_e, v	0.5	1.0 to 2.3
Estimated ionization fraction, n_e/n	0.1 to 1.0	0.01 to 0.1
Tip temperature (pyrometer), °K	1600	1350

[a] For region between cathode and anode.

For both modes the potential was nearly constant over the main body of the discharge (Fig. 2a) at about 11 v above the cathode. This value barely exceeds the first ionization potential of mercury (10.4 v). The edge of this nearly equipotential plateau (where the potential gradient becomes appreciable) will be called the "sheath edge." In these experiments no probe measurements could be made closer than 0.3 cm to the cathode; thus the position of the sheath edge could only be inferred. For a hollow cathode of the type described, it is clear that if the sheath dimension is large compared with the orifice, it will envelop the front surface of the tip, and the geometry of the hole would have little influence on its shape. On the other hand, if the sheath dimension is much smaller than the orifice radius, the sheath may line the contours of the cathode everywhere, including the inside of the orifice channel and the cavity.

A high estimate of the Debye length for conditions that appear to exist inside the hollow cathode in the spot mode is 7×10^{-6} m, which is ~3% of the orifice diameter. In the plume mode the estimated Debye length is $\sim 3 \times 10^{-5}$ m, approaching the order of magnitude of the orifice dimensions. This suggests that the spot mode is characterized by the sheath edge deep inside the cavity, while the plume mode has a sheath spanning the orifice on the outside as indicated in Fig. 3.

In the spot mode, according to this model, electrons accelerated through the sheath are projected into the inner region of the cathode. This mechanism explains—at least qualitatively—the higher electron density (thus higher degree of ionization) observed in this mode. Moreover, since most fast electrons produce ionization or excitation and lose their energy inside or very near the tip, the larger portion of the discharge region between cathode and anode is not luminous.

For the plume mode, if the sheath edge is assumed to lie outside the cathode as in the proposed model, it can be shown[4] that only a small portion of the electrons that have been accelerated through the sheath will undergo ionizing collisions. Thus fast electrons are present in the discharge and apparently make enough excitation collisions to give luminousity to the plume.

These investigations indicate then that the two principal modes of operation of the hollow cathode are probably associated with different sheath configurations near the cathode. It is hoped that the plasma parameter data presented in this Note will contribute to the understanding of the mechanisms of the discharge in these modes.

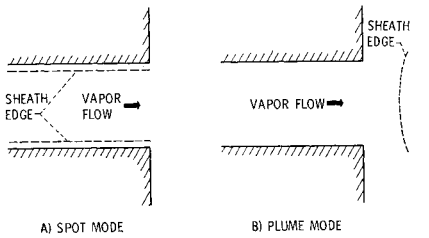

Fig. 3 Hypothetical sheath-edge positions in orifice channel cross section.

References

[1] Kerslake, W. R., Byers, D. C., and Staggs, J. F., "SERT II Experimental Thruster System," AIAA Paper 67-700, New York, 1967.

[2] Rawlin, V. K. and Pawlik, E. V., "A Mercury Plasma-Bridge Neutralizer," AIAA Paper 67-670, New York, 1967.

[3] Bechtel, R. T., Csiky, G. A., and Byers, D. C., "Performance of a 15-Centimeter Diameter, Hollow-Cathode Kaufman Thruster," AIAA Paper 68-88, New York, 1968.

[4] Csiky, G. A., "Measurements of Some Properties of a Discharge from a Hollow Cathode," TN D-4966, 1969, NASA.

Linearized Impulsive Earth-Approach Guidance Analysis

THOMAS B. MURTAGH*
NASA Manned Spacecraft Center, Houston, Texas

Introduction

REFERENCES 1–5 discuss the linear theory of impulsive velocity corrections for space vehicle guidance, but the discussions are restricted to fixed-time-of-arrival (FTA) and variable-time-of-arrival (VTA) position guidance, with no attempt to generalize the formulation of the guidance laws. A similarity of form among the guidance laws is evident, which suggests that the laws somehow are related mathematically. Cicolani[6] noted the similarity and attempted to determine the general properties of linearized impulsive guidance laws by using the concepts of linear vector spaces and the pseudoinverse of a matrix. A more straight-forward approach to the problem was made by Tempelman,[7] who started with a generalized linear constraint equation and developed a general solution to the impulsive guidance problem. Ribarich and Meredith[8] have shown that the theory of maxima and minima is another convenient framework for formulating problems in the midcourse guidance area.

The analysis presented in this Note originally was motivated by Tempelman's work and is an attempt to delineate certain types of terminal constraints affecting the particular matrices comprising the general linear impulsive guidance law. A comparison of a variety of guidance laws for the Earth approach phase of a representative conjunction-class Mars mission is presented to illustrate the theory.

Received April 25, 1969; revision received November 14, 1969.

* Aerospace Engineer. Member AIAA.

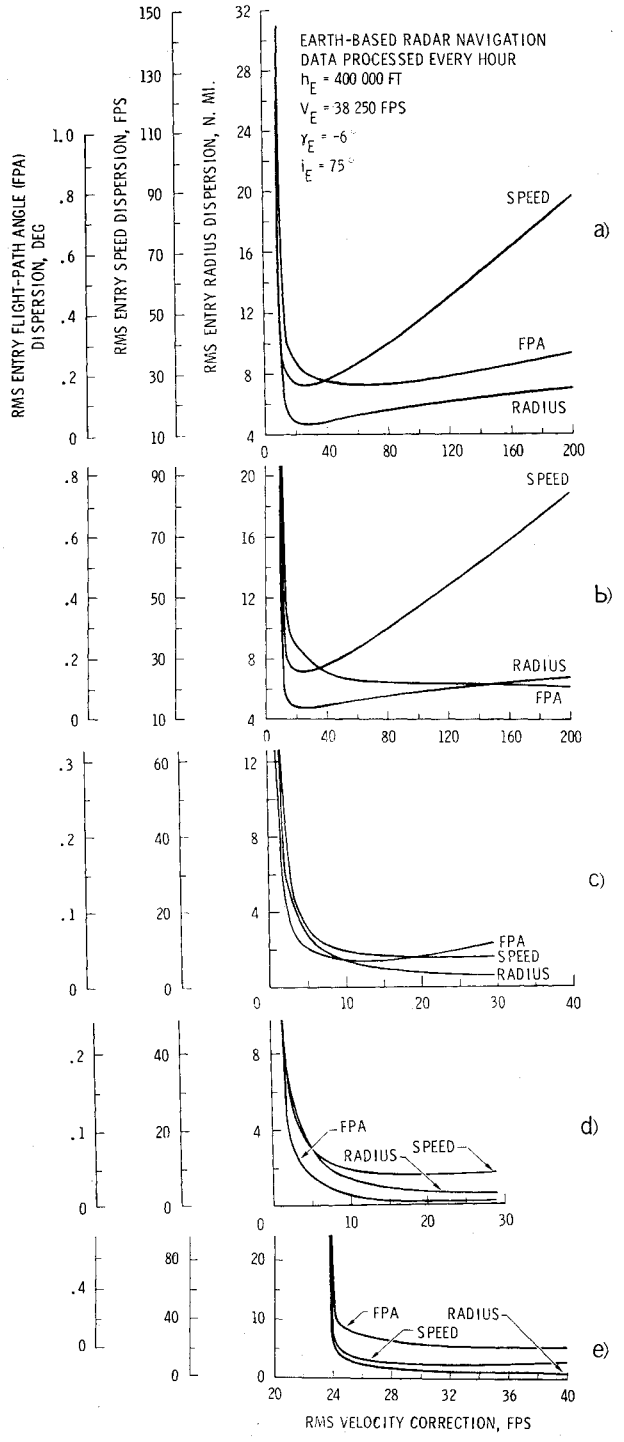

Fig. 1 Comparison of dispersions for fixed time of arrival guidance: a) FTA, null position vector errors, b) FTA, null radial, cross-range, and flight-path angle errors, and variable time of arrival guidance, c) VTA, null position vector errors, minimize ΔV, d) VTA, null radial, cross-range, and flight-path angle errors, minimize ΔV, e) VTA, null radial, cross-range, and flight-path angle errors, minimize distance to nominal entry interface.

Analysis

Equation for the velocity correction

The velocity correction $\Delta\bar{V}(t)$ is defined by

$$\Delta\bar{V}(t) = \delta\bar{V}^{+}(t) - \delta\bar{V}^{-}(t) \tag{1}$$

where the superscripts (—) and (+) denote quantities before and after the maneuver, respectively. Equation (1) can also be written[7]

$$\Delta\bar{V}(t) = -K^{-1}H\delta\bar{R}^{-}(t) - \delta\bar{V}^{-}(t) - K^{-1}\bar{L}\delta\tau \tag{2}$$

The equation for $\delta\tau$, the variation in the nominal time of arrival, may be cast into either of the following forms

$$\delta\tau = \bar{\alpha}_1{}^T\delta\bar{R}^{-}(t) + \bar{\beta}_1{}^T\delta\bar{V}^{+}(t) \tag{3}$$

or

$$\delta\tau = \bar{\alpha}_2{}^T\delta\bar{R}^{-}(t) + \bar{\beta}_2{}^T\delta\bar{V}^{-}(t) \tag{4}$$

where the superscript T denotes the transpose operator.

Substitution of the appropriate equation for $\delta\tau$ into Eq. (2) produces an expression for $\Delta\bar{V}(t)$ of the form[4,6]

$$\Delta\bar{V}(t) = G_1\delta\bar{R}^{-}(t) + G_2\delta\bar{V}^{-}(t) \tag{5}$$

where G_1 and G_2 are submatrices of the guidance law matrix[4,6]

$$G = \begin{bmatrix} 0 & 0 \\ G_1 & G_2 \end{bmatrix} \tag{6}$$

Fixed-time-of-arrival guidance laws

The most commonly used FTA guidance law ($\delta\tau = 0$) imposes the constraints

$$d\bar{R}^{+}(\tau) = 0 \tag{7}$$

and is referred to as FTA position guidance.[1-4] The matrices G_1 and G_2 for this guidance law are

$$G_1 = -\phi_2{}^{-1}\phi_1, \quad G_2 = -I \tag{8}$$

where ϕ_2 and ϕ_1 are submatrices of the transition matrix[1]

$$\phi(\tau,t) = \begin{bmatrix} \phi_1 & \phi_2 \\ \phi_3 & \phi_4 \end{bmatrix} \tag{9}$$

and I is the identity matrix. Another type of FTA guidance law might constrain the radial, cross-range, and flightpath angle errors at the terminal time τ. The radial error is defined as the component of the position error along the radius vector; the cross-range error is defined as the component of the position error along the orbital angular momentum vector $\bar{h}$. The constraint equations are

$$\bar{R}^T(\tau)\delta\bar{R}^{+}(\tau) = 0 \tag{10}$$

$$\bar{h}^T(\tau)\delta\bar{R}^{+}(\tau) = 0 \tag{11}$$

$$\bar{\eta}^T(\tau)\delta\bar{V}^{+}(\tau) - \bar{V}^T(\tau)\delta\bar{R}^{+}(\tau) = 0 \tag{12}$$

where

$$\bar{\eta}(\tau) = [(\bar{R} \times \bar{V}) \times \bar{V}]/V^2 \tag{13}$$

The expressions for the matrices K and H in Eq. (2) are

$$K = \begin{bmatrix} \bar{\eta}^T\phi_4 - \bar{V}^T\phi_2 \\ \bar{R}^T\phi_2 \\ \bar{h}^T\phi_2 \end{bmatrix} \quad H = \begin{bmatrix} \bar{\eta}^T\phi_3 - \bar{V}^T\phi_1 \\ \bar{R}^T\phi_1 \\ \bar{h}^T\phi_1 \end{bmatrix} \tag{14}$$

The matrices G_1 and G_2 are readily shown to be

$$G_1 = -K^{-1}H, \quad G_2 = -I \tag{15}$$

Other types of FTA guidance laws can be generated by imposing the appropriate terminal constraints and casting the final expression in the form of Eq. (5). Stern[2] develops FTA guidance laws which are derived by imposing constraints on certain combinations of the Keplerian orbital elements.

Variable-time-of-arrival guidance laws

The most commonly used VTA guidance law constrains the radial and cross-range components of the position vector error at the terminal time τ and computes $\delta\tau$ to minimize the magnitude of the commanded velocity correction.[3,4,6] A similar VTA guidance law is constructed by imposing the constraints in Eqs. (10–12) to produce the expression for K and H in Eq. (14), and the following equation for the vector $\bar{L}$ required for

Eq. (2)

$$\bar{L} = \begin{bmatrix} \bar{\eta}^T\bar{a} - \bar{V}^T\bar{V} \\ \bar{R}^T\bar{V} \\ 0 \end{bmatrix} \quad (16)$$

where $\bar{a}$ is the acceleration at the terminal time τ. For this guidance law,

$$G_1 = G_2K^{-1}H,\ G_2 = [\bar{c}\bar{c}^T/\bar{c}^T\bar{c}] - I \quad (17)$$

and the vector $\bar{c}$ is defined by

$$\bar{c} = K^{-1}\bar{L} \quad (18)$$

The constraints represented by Eqs. (10–12) also may be used to construct a VTA guidance law which computes $\delta\tau$ to minimize the distance from the nominal target point.[7]

Results and Discussion

The reference trajectory chosen to illustrate the guidance laws outlined in the preceding sections is a 1977 Mars-orbital mission discussed in considerable detail in Ref. 9. The maneuver required to target the spacecraft to the entry corridor is assumed to be executed at the Earth sphere of influence (SOI). The assumed imperfect execution of this maneuver necessitates the subsequent midcourse maneuvers, which are the subject of this Note. The position and velocity uncertainties at the time of this maneuver are 300 naut miles and 1 fps; the corresponding dispersions are 900 naut miles and 8 fps. The nominal entry conditions are an altitude h_E of 400,000 ft and flight path angle γ_E of $-6°$, which result in an entry speed V_E of 38,250 fps. The time required for the spacecraft to reach the Earth-entry interface from the Earth SOI is 64 hr. The inclination of the entry trajectory i_E is 75°.

The root-mean-square (rms) entry radius, speed, and flight path angle dispersions are presented in Fig. 1 as a function of the rms midcourse ΔV. The midcourse maneuever execution errors are assumed to be a 1% proportional error, a 1° pointing error, and a $\frac{1}{2}$-fps engine cut-off error.[4] Earth based radar measurements were assumed to be made once per hour.

In Fig. 1a, the FTA guidance law is formulated to null position vector errors at the nominal time of arrival at the entry interface. This figure is indicative of an optimum time to execute the midcourse maneuver and produce minimum values of the entry parameter dispersions for the smallest propellant expenditure. However, the optimum time for minimum dispersion is different for each of the entry parameters. The techniques discussed in Ref. 10 could be used to determine analytically the optimum single correction times, but such a determination is beyond the scope of this Note.

In Fig. 1b, the FTA guidance law is formulated to null radial, cross-range, and γ_E errors at the nominal time of arrival at the entry interface. As might be expected, the γ_E control is better for this guidance law.

The dispersions for the VTA guidance laws are presented in Figs. 1c–1e. The entry-speed errors are generally lower than the corresponding errors for the FTA guidance laws, but these differences are misleading, because, for the VTA guidance laws, an associated plot of the rms timing error (data not shown) maps into a velocity error, and this velocity error, in effect, must be added to the speed error computed from the VTA guidance equations. For the VTA guidance laws considered typical timing errors are 150–300 sec. However, the relaxation of the constraint on the time of arrival permits a smaller rms ΔV requirement for specified radius and γ_E errors. For the trajectory considered (which is representative of a conjunction-class Mars mission), the best over-all performance is produced by the guidance law which is formulated to null radial, cross-range, and γ_E errors while the magnitude of the commanded ΔV is minimized (Fig. 1d).

References

[1] Battin, R. H., *Astronautical Guidance*, McGraw-Hill, New York, 1964.

[2] Stern, R. G., "Interplanetary Midcourse Guidance Analysis," Vol. 1, CR-51827, 1964, NASA.

[3] White, J. S., Callas, G. P., and Cicolani, L. S., "Application of Statistical Filter Theory to the Interplanetary Navigation and Guidance Problem," TN D-2697, 1965, NASA.

[4] Murtagh, T. B., Lowes, F. B., and Bond, V. R., "Navigation and Guidance Analysis of a Mars Probe Launched from a Manned Flyby Spacecraft," TN D-4512, 1968, NASA.

[5] Robbins, H. M., "An Analytical Study of the Impulsive Approximation," *AIAA Journal*, Vol. 4, No. 8, Aug. 1966, pp. 1417–1423.

[6] Cicolani, L. S., "Linear Theory of Impulsive Velocity Corrections for Space Mission Guidance," TN D-3365, 1966, NASA.

[7] Tempelman, W., "Linearized Impulsive Guidance Laws," *AIAA Journal*, Vol. 3, No. 11, Nov. 1965, pp. 2148–2149.

[8] Ribarich, J. J. and Meredith, C. M., "Analysis of Surveyor Midcourse Guidance as a Problem in the Theory of Maxima and Minima," *Journal of Spacecraft and Rockets*, Vol. 3, No. 7, July 1966, pp. 997–1001.

[9] Lowes, F. B. and Murtagh, T. B., "Navigation and Guidance Systems Performance for Three Typical Manned Interplanetary Missions," TN D-4629, 1968, NASA.

[10] Murtagh, T. B., "Optimum Interplanetary Midcourse Velocity-Correction Schedules," *Proceedings of the Fourth Congress of the International Federation of Automatic Control*, Warsaw, Poland, 1969, pp. 19–38; also *The IFAC Journal, Automatica*, Pergamon Press, New York, Vol. 6, No. 1, Jan. 1970, pp. 99–109.

Low-Thrust Mission Simulation–Feedback to Hardware Definition

ALFRED C. MASCY*

NASA Ames Research Center, Moffett Field, Calif.

AMONG the major functional elements of solar and nuclear electric propulsion mission simulation are the representation of the high- and low-thrust planetocentric and heliocentric trajectories, and the necessary definition of the powerplant, thruster, and power-conditioning characteristics. There is always interplay between the elements, and each has its unique role in the over-all optimization criteria. Mission analyses should provide feedback to the hardware developers, and vice versa. Feedback effects for two levels of sophistication are indicated in Fig. 1. A computer program along these lines is presently being developed.[1] This Note briefly describes the approach and presents some examples of the influences of powerplant and thruster characteristics for unmanned Saturn orbiter missions.

Returning to Fig. 1, high- and low-thrust trajectory optimization may be accomplished by rapid, level 1 type routines or by higher precision, level 2 type routines. Level 1 modules use functional relationships for the energy requirements of precomputed optimum trajectories obtained from accurate computer programs.[2] Curve-fitting procedures have been employed to define the energy parameter, J, as a function of time and hyperbolic excess velocity V_∞ at Earth departure and planet arrival. A method of system optimization, based on the invariance of J with system parameters, was found to be quite accurate.[3] Low-thrust planetocentric operations are expressed analytically, em-

Presented at the AIAA 7th Electric Propulsion Conference, Williamsburg, Va., March 3–5, 1969 (no paper number; published in bound volume of conference papers); submitted April 28, 1969; revision received February 18, 1970.

* Research Scientist, Mission Analysis Division, Office of Advanced Research and Technology. Member AIAA.